

Electronic exchange in quantum rings: Beyond the local-density approximation

E. Räsänen,^{1,2,3,*} S. Pittalis,^{1,3,†} C. R. Proetto,^{1,3} and E. K. U. Gross^{1,3}

¹*Institut für Theoretische Physik, Freie Universität Berlin, Arnimallee 14, D-14195 Berlin, Germany*

²*Nanoscience Center, Department of Physics, University of Jyväskylä, P.O. Box 35, FI-40014 Jyväskylä, Finland*

³*European Theoretical Spectroscopy Facility (ETSF)*

(Received 7 December 2008; published 13 March 2009)

Quantum rings can be characterized by a specific radius and ring width. For this rich class of physical systems, an accurate approximation for the exchange-hole potential and thus for the exchange energy is derived from first principles. Excellent agreement with the exact-exchange results is obtained regardless of the ring parameters, total spin, current, or the external magnetic field. The description can be applied as a density functional outperforming the commonly used local spin-density approximation, which is here explicitly shown to break down in the quasi-one-dimensional limit. The dimensional crossover, which is of extraordinary importance in low-dimensional systems, is fully captured by our functional.

DOI: 10.1103/PhysRevB.79.121305

PACS number(s): 73.21.La, 71.15.Mb

Ring-shaped quantum systems such as semiconductor quantum rings (QRs) have attracted wide interest both theoretically and experimentally. Presently, QRs can be fabricated using a variety of techniques.^{1–3} The tunabilities of size, shape, and electron number in QRs suggest applications in the field of quantum-information technology. In particular, one can exploit the well-known Aharonov-Bohm effect⁴ by external magnetic fields⁵ or control the electronic states by short laser pulses within the decoherence time.⁶

Many-electron QRs have been studied theoretically using various approaches, e.g., model Hamiltonians,^{7,8} exact diagonalization,^{9,10} quantum Monte Carlo,^{10,11} and density-functional theory (DFT) (Refs. 12–14). Within spin-DFT (SDFT) or current-SDFT applied to QRs, the exchange and correlation energies and potentials are commonly calculated using the two-dimensional (2D) local spin-density approximation (LSDA) (Ref. 15). For relatively wide QRs, LSDA performs reasonably well,^{12–14} which is not surprising in view of the good performance of the LSDA in the case of 2D quantum dots.¹⁶ However, in the quasi-one-dimensional (quasi-1D) limit the 2D-LSDA is expected to fail similarly to the breakdown of the three-dimensional LSDA in the quasi-2D limit.¹⁷ Hence, in order to benefit from the efficiency of DFT methods in various QRs, accurate density functionals for exchange and correlation are needed. Methods based on exact-exchange (EXX) functional seem an attractive possibility.¹⁸ However, most computational schemes exploiting EXX for finite systems suffer from numerical problems,^{18,19} which, ultimately, prevents the method from being applied to large electron numbers.

In this Rapid Communication we derive an accurate method to calculate the exchange-hole potential and the exchange energy of QRs. The resulting density functional is simpler than EXX but yet compatible with correlation functionals based on the modeling of the correlation hole.²⁰ Our derivation follows the strategy originally proposed for atoms by Becke and Roussel,²¹ in which the averaged exchange hole of a suitable single-electron wave function is adapted to a general N -electron system by examining the short-range behavior of the exchange hole. Recently, a similar approach has been used to develop exchange functionals for finite 2D systems,²² which can be reproduced as a special case of this

work. In the numerical examples we demonstrate the accuracy of the functional against EXX results and underline the considerable improvement over the LSDA, particularly in the quasi-1D limit.

In the framework of SDFT the exact exchange-energy functional of the spin densities $\rho_{\uparrow}(\mathbf{r})$ and $\rho_{\downarrow}(\mathbf{r})$ can be written in effective atomic units²³ (eff. a.u.) as

$$E_x[\rho_{\uparrow}, \rho_{\downarrow}] = -\frac{1}{2} \sum_{\sigma=\uparrow, \downarrow} \int d\mathbf{r}_1 \int d\mathbf{r}_2 \frac{\rho_{\sigma}(\mathbf{r}_1)}{|\mathbf{r}_1 - \mathbf{r}_2|} h_x^{\sigma}(\mathbf{r}_1, \mathbf{r}_2), \quad (1)$$

where

$$h_x^{\sigma}(\mathbf{r}_1, \mathbf{r}_2) = \frac{\left| \sum_{k=1}^{N_{\sigma}} \psi_{k,\sigma}^*(\mathbf{r}_1) \psi_{k,\sigma}(\mathbf{r}_2) \right|^2}{\rho_{\sigma}(\mathbf{r}_1)} \quad (2)$$

is the exchange-hole function. Here we assume that the non-interacting ground state is nondegenerate and hence takes the form of a single Slater determinant constructed from the Kohn-Sham (KS) orbitals, $\psi_{k,\sigma}$.

Next we look for an approximation for the *cylindrical* average of the exchange hole. It is defined around \mathbf{r}_1 with respect to $\mathbf{s} = \mathbf{r}_2 - \mathbf{r}_1$ as²²

$$\bar{h}_x^{\sigma}(\mathbf{r}_1, s) = \frac{1}{2\pi} \int_0^{2\pi} d\phi_s h_x^{\sigma}(\mathbf{r}_1, \mathbf{r}_1 + \mathbf{s}). \quad (3)$$

In the following, we compute \bar{h}_x^{σ} *exactly* for a single-electron wave function of a QR. We consider a 2D QR defined by a radial confining potential of the form²⁴

$$V(r) = \frac{M^2}{2r^2} + \frac{\alpha^4}{2} r^2 - M\alpha^2, \quad (4)$$

where $M \geq 0$ and $\alpha > 0$ are constants. Note that $M=0$ corresponds to a harmonic quantum dot.¹⁶ Regarding QR fabrication,^{1–3} the confinement given above is realistic: on one hand, the electrons cannot enter the center area described by the strongly peaked “antidot” [first term in $V(r)$] and on the other hand, the edge of the QR is described by a soft parabolic confinement [second term in $V(r)$]. In this tunable

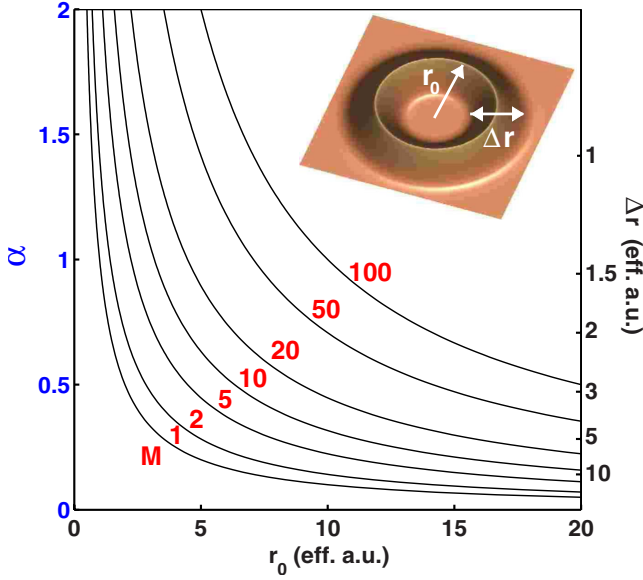


FIG. 1. (Color online) Relation between the parameter set (α, M) in the external confining potential [Eq. (4)] and the single-electron ring radius r_0 and width Δr (see the inset). The curves correspond to fixed values of M .

model, both the radius and width of the QR can be changed independently by varying M and α (see below).

The eigenfunctions and eigenvalues for a single-electron confined by $V(r)$ in Eq. (4) can be solved analytically.²⁴ Setting the radial and angular quantum numbers to zero yields a wave function,

$$\psi_\alpha(\mathbf{r}) = \frac{\alpha^{M+1}}{\sqrt{\pi M!}} r^M e^{-\alpha^2 r^2/2}. \quad (5)$$

We emphasize that this expression, normalized for each α and M , is the *general* single-electron ground-state wave function of a QR having a potential minimum at $r=r_0 = \sqrt{M}/\alpha$, which corresponds to the ring radius. The width of the single-electron QR having the energy $E_0 = \alpha^2$ can be approximated by $\Delta r = \sqrt{2}/\alpha$. In Fig. 1 we show explicitly the relation between the *single-electron* radius and width of the QR $(r_0, \Delta r)$ and the parameters (M, α) in the external confining potential given in Eq. (4).

The exact exchange-hole function for the single-electron wave function in Eq. (5) becomes

$$h_{x,1}^\sigma(\mathbf{r}_1, \mathbf{r}_2) = \psi_\sigma^*(\mathbf{r}_2) \psi_\sigma(\mathbf{r}_2) = \rho_\sigma(\mathbf{r}_2) = \frac{\alpha^{2(M+1)}}{\pi M!} r_2^{2M} e^{-\alpha^2 r_2^2}. \quad (6)$$

To calculate the cylindrical average as defined in Eq. (3), we first set $\mathbf{r}_1 = \mathbf{r}$ and $\mathbf{r}_2 = \mathbf{r} + \mathbf{s}$. As a result we get

$$\bar{h}_{x,1}^\sigma(\mathbf{r}, \mathbf{s}) = \frac{1}{2\pi} \int_0^{2\pi} d\phi_s \rho_\sigma(\mathbf{r} + \mathbf{s}) = \frac{\alpha^{2(M+1)}}{\pi M!} e^{-\alpha^2(r^2+s^2)} (r^2+s^2)^M \times \sum_{k=0}^M (-1)^k \binom{M}{k} \left(\frac{2rs}{r^2+s^2} \right)^k \frac{d^k}{dz^k} I_0(z) \Big|_{z=2\alpha^2 rs}, \quad (7)$$

where $I_0(z)$ is the zeroth-order modified Bessel function of

the first kind and M is now an integer (see below).

Next, we apply $\bar{h}_{x,1}^\sigma$ as a general model for the averaged exchange hole of an N -electron system.^{21,22} The model is required to locally reproduce the short-range behavior of the exchange hole. Therefore, we parametrize α^2 and r^2 into functions of r by setting $\alpha^2 \rightarrow a(r)$ and $r^2 \rightarrow b(r)$. Equation (7) can now be rewritten as

$$\bar{h}_x^\sigma(a, b; s) = \frac{a^{M^*+1}}{\pi M^*!} e^{-a(b+s^2)} (b+s^2)^{M^*} \sum_{k=0}^{M^*} (-1)^k \binom{M^*}{k} \times \left(\frac{2\sqrt{b}s}{b+s^2} \right)^k \frac{d^k}{dz^k} I_0(z) \Big|_{z=2a\sqrt{b}s}, \quad (8)$$

where $M^* = 2(\Delta r^*/r_0^*)^{-2}$ is the nearest integer describing the characteristic ratio between the effective width and the radius of the N -electron QR. As we will show below, r_0^* and Δr^* can be extracted from the spin density. As a consequence, M^* can be considered as a (spin) density functional $M^*[\rho_\sigma]$. The short-range behavior of the exact exchange hole with respect to s can be obtained from the first two nonvanishing terms in the Taylor expansion in Eq. (3):

$$\bar{h}_x^\sigma(\mathbf{r}, s) = \rho_\sigma(\mathbf{r}) + s^2 C_x^\sigma(\mathbf{r}) + \dots, \quad (9)$$

where

$$C_x^\sigma = \frac{1}{4} \left[\nabla^2 \rho_\sigma - 2\tau_\sigma + \frac{1}{2} \frac{(\nabla \rho_\sigma)^2}{\rho_\sigma} + 2 \frac{\mathbf{j}_{p,\sigma}^2}{\rho_\sigma} \right] \quad (10)$$

is the local curvature of the exchange hole in 2D (Ref. 22) around the given reference point \mathbf{r} (argument omitted). Here the (double of the) kinetic-energy density, $\tau_\sigma = \sum_{k=1}^{N_\sigma} |\nabla \psi_{k,\sigma}|^2$, and the spin-dependent paramagnetic current density, $\mathbf{j}_{p,\sigma} = \frac{1}{2i} \sum_{k=1}^{N_\sigma} [\psi_{k,\sigma}^* (\nabla \psi_{k,\sigma}) - (\nabla \psi_{k,\sigma}^*) \psi_{k,\sigma}]$, depend explicitly on the KS orbitals and hence implicitly on the spin densities. Defining $y(r) := a(r)b(r)$, the zeroth-order term in Eq. (9) yields

$$\rho_\sigma = \frac{a}{\pi M^*!} y^{M^*} e^{-y}, \quad (11)$$

and the second-order term gives

$$C_x^\sigma = \frac{a^2}{\pi M^*!} y^{M^*-1} [(y - M^*)^2 - y] e^{-y}. \quad (12)$$

Combining Eqs. (11) and (12) leads to

$$M^*! y^{-(M^*+1)} [(y - M^*)^2 - y] e^y = \frac{C_x^\sigma}{\pi \rho_\sigma^2}, \quad (13)$$

from which y can be solved numerically. Now, we can compute a and b and thus the averaged exchange hole from Eq. (8). The exchange-hole potential is given by

$$U_x^\sigma(\mathbf{r}) = -2\pi \int_0^\infty ds \bar{h}_x^\sigma(a, b; s), \quad (14)$$

from which the exchange energy can be calculated as

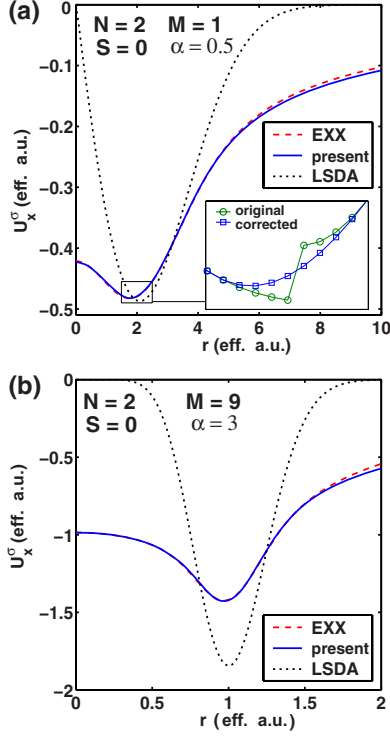


FIG. 2. (Color online) Exchange-hole potentials of two-electron quantum rings (total spin $S=0$) defined by parameters (a) $M=1$, $\alpha=0.5$, and (b) $M=9$, $\alpha=3$. The dashed line shows the EXX result, the solid line is the result of the present work, and the dotted line corresponds to the LSDA result.

$$E_x[\rho_\uparrow, \rho_\downarrow] = \frac{1}{2} \sum_{\sigma} \int d\mathbf{r} \rho_{\sigma}(\mathbf{r}) U_x^{\sigma}(\mathbf{r}). \quad (15)$$

From Eqs. (8) and (14) it can be shown that our calculation scheme preserves also the exact long-range behavior: $U_x^{\sigma}(r \rightarrow \infty) \rightarrow -1/r$.

To summarize our method, the calculation of the exchange energy of an N -electron QR consists of the following steps.

- (1) Use the KS orbitals $\psi_{k,\sigma}$ to calculate the spin densities ρ_{σ} , the local curvature of the exchange hole C_x^{σ} from Eq. (10), and to estimate M^* .
- (2) Compute $y(r)$ numerically from Eq. (13).
- (3) Calculate $a(r)$ from Eq. (11) and $b(r)$ from the relation $b(r)=y(r)/a(r)$.
- (4) Calculate the averaged exchange-hole function from Eq. (8).
- (5) Finally calculate the exchange-hole potential and the exchange energy from Eqs. (14) and (15), respectively.

Next we test the performance of our functional in a few examples. As the reference results we use the exchange-hole potentials and exchange energies of the EXX calculations within the rather accurate Krieger-Li-Iafrate (KLI) approximation.²⁵ We compare the results also to the 2D-LSDA exchange.²⁶ Both the EXX and LSDA results are obtained using the OCTOPUS code.²⁷ The converged EXX orbitals are used as the input KS orbitals in our functional (and in the LSDA). Alternatively, also the LSDA orbitals can be

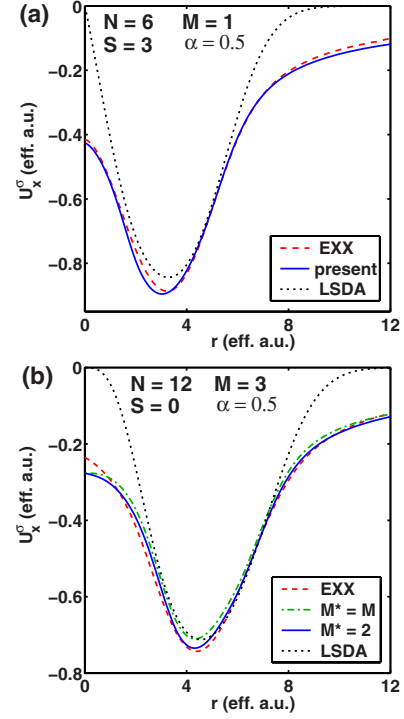


FIG. 3. (Color online) Same as in Fig. 2 but for (a) a fully spin-polarized current-carrying six-electron quantum ring at $B=6$ T and for (b) a zero-current 12-electron quantum ring.

used as input, which in most cases lead to only minor changes in the results.

Figure 2 shows the exchange-hole potentials for two-electron singlet states of two QRs defined by (a) $(M, \alpha) = (1, 0.5)$ and (b) $(M, \alpha) = (9, 3)$, respectively. Note that here we have set $M^*=M$ as the first approximation. In both cases we find excellent agreement between the EXX (dashed lines) and the present work (solid lines). Both the large- r limit, where U_x^{σ} decays as $-1/r$, and the $r \rightarrow 0$ limit are correctly reproduced.

The exchange energies per particle of the LSDA (dotted lines in Fig. 2), which are directly comparable to U_x^{σ} , deviate significantly from the EXX and from our approximation. The inability of the LSDA to yield the correct shape of the curve is due to the simple density-dependent expression of the exchange energy per particle in the LSDA, i.e., $\epsilon_{x,\sigma}^{\text{LSDA}} \propto \rho_{\sigma}^{1/2}$, leading to differences also in the exchange energy. In the case of Fig. 2(a), we find $E_x^{\text{LSDA}} = -0.389$, whereas $E_x^{\text{EXX}} = -0.409$ and $E_x^{\text{present}} = -0.408$. When the ratio $\Delta r/r_0$ is decreased to one third, i.e., $M=1 \rightarrow 9$, the deviation of the LSDA becomes more pronounced as shown in Fig. 2(b). Now we find $E_x^{\text{LSDA}} = -1.502$ vs $E_x^{\text{EXX}} = E_x^{\text{present}} = -1.300$. In other words, the above change in M increases the relative error of the LSDA exchange energy from 5 to 16%. Hence, these results demonstrate the breakdown of the 2D-LSDA in the quasi-one-dimensional limit.

At this point we make two remarks on the numerical procedure. First, Eq. (13) has two solutions for $y(r)$, from which we choose the smaller one for $r < r[\rho_{\text{max}}]$ and the larger one otherwise. Since these two solutions do not generally coincide at $r = r[\rho_{\text{max}}]$, we extrapolate $U_x^{\sigma}(r)$ around this point as

visualized in the inset of Fig. 2. This smoothing procedure is done such that E_x is not altered. Second, the application of the overall scheme might be numerically cumbersome in the small- r regime when M (and/or M^*) is large and the density is very small. To overcome this problem, we take the advantage of the exact property of our model, $U_x^\sigma(r \rightarrow 0) = -(2M)!(M!)^{-2}2^{-2M}\alpha\sqrt{\pi} + O(r^2)$, which is valid for a general N -electron case with $M > 1$.

To demonstrate the generality of our method, we show in Fig. 3 the exchange-hole potentials for (a) a spin-polarized current-carrying six-electron QR at $B=6$ T and for (b) a 12-electron QR. Similarly to the previous examples, we find excellent agreement with the EXX. The six-electron case yields $E_x^{\text{EXX}} = -2.226$, $E_x^{\text{present}} = -2.238$, and $E_x^{\text{LSDA}} = -2.114$. In the case of 12 electrons, we plot results for both $M^* = M = 3$ and for $M^*[\rho] = 2 \approx 2(\Delta r^*/r_0^*)^{-2}$, where the effective radius r_0^* corresponds to the point where the cumulative density reaches 50%, and the effective width Δr^* , centered at r_0^* , covers 90% of the total density. We find that in the latter case the agreement with the EXX is better.

To conclude, we have derived, from first principles, an accurate and general approximation for the exchange-hole potential and hence for the exchange energy in quantum rings. Excellent agreement with the exact-exchange results is obtained regardless of the ring geometry, number of electrons, spin polarization, and currents. Moreover, we have demonstrated that, in contrast to the local-density approximation, our functional can deal with the physically relevant dimensional crossover between two and one dimensions. Our approach is suitable for the development of correlation functionals by considering the exact properties of the corresponding correlation-hole potentials.²⁰

This work was supported by the Deutsche Forschungsgemeinschaft, the EU's Sixth Framework Programme through the Nanoquanta Network of Excellence (Grant No. NMP4-CT-2004-500198), and the Academy of Finland. C.R.P. was supported by the European Community through a Marie Curie IIF (Grant No. MIF1-CT-2006-040222) and CONICET of Argentina through Grant No. PIP 5254.

*esa.rasanen@jyu.fi

†pittalis@physik.fu-berlin.de

¹A. Lorke, R. J. Luyken, A. O. Govorov, J. P. Kotthaus, J. M. Garcia, and P. M. Petroff, Phys. Rev. Lett. **84**, 2223 (2000).

²A. Fuhrer, S. Lüscher, T. Ihn, T. Heinzel, K. Ensslin, W. Wegscheider, and M. Bichler, Nature (London) **413**, 822 (2001).

³U. F. Keyser, C. Fühner, S. Borck, R. J. Haug, M. Bichler, G. Abstreiter, and W. Wegscheider, Phys. Rev. Lett. **90**, 196601 (2003).

⁴Y. Aharonov and D. Bohm, Phys. Rev. **115**, 485 (1959).

⁵See, e.g., M. Sigrist, A. Fuhrer, T. Ihn, K. Ensslin, S. E. Ulloa, W. Wegscheider, and M. Bichler, Phys. Rev. Lett. **93**, 066802 (2004).

⁶E. Räsänen, A. Castro, J. Werschnik, A. Rubio, and E. K. U. Gross, Phys. Rev. Lett. **98**, 157404 (2007).

⁷S. Viefers, P. Koskinen, P. Singha Deo, and M. Manninen, Physica E (Amsterdam) **21**, 1 (2004).

⁸M. M. Fogler and E. Pivovarov, Phys. Rev. B **72**, 195344 (2005).

⁹K. Niemelä, P. Pietiläinen, P. Hyvönen, and T. Chakraborty, Europhys. Lett. **36**, 533 (1996).

¹⁰S. S. Gylfadottir, A. Harju, T. Jouttenus, and C. Webb, New J. Phys. **8**, 211 (2006).

¹¹A. Emperador, F. Pederiva, and E. Lipparini, Phys. Rev. B **68**, 115312 (2003).

¹²A. Emperador, M. Pi, M. Barranco, and E. Lipparini, Phys. Rev. B **64**, 155304 (2001).

¹³M. Aichinger, S. A. Chin, E. Krotscheck, and E. Räsänen, Phys. Rev. B **73**, 195310 (2006).

¹⁴E. Räsänen and M. Aichinger, J. Phys.: Condens. Matter **21**, 025301 (2009).

¹⁵C. Attaccalite, S. Moroni, P. Gori-Giorgi, and G. B. Bachelet,

Phys. Rev. Lett. **88**, 256601 (2002).

¹⁶For a review, see, e.g., L. P. Kouwenhoven, D. G. Austing, and S. Tarucha, Rep. Prog. Phys. **64**, 701 (2001); S. M. Reimann and M. Manninen, Rev. Mod. Phys. **74**, 1283 (2002).

¹⁷Y.-H. Kim, I.-H. Lee, S. Nagaraja, J.-P. Leburton, R. Q. Hood, and R. M. Martin, Phys. Rev. B **61**, 5202 (2000); L. Pollack and J. P. Perdew, J. Phys.: Condens. Matter **12**, 1239 (2000).

¹⁸N. Helbig, S. Kurth, S. Pittalis, E. Räsänen, and E. K. U. Gross, Phys. Rev. B **77**, 245106 (2008).

¹⁹See, e.g., T. Heaton-Burgess, F. A. Bulat, and W. Yang, Phys. Rev. Lett. **98**, 256401 (2007); V. N. Staroverov and G. E. Scuseria, J. Chem. Phys. **124**, 141103 (2006); **125**, 081104 (2006); D. R. Rohr, O. V. Gritsenko, and E. J. Baerends, J. Mol. Struct.: THEOCHEM **72**, 762 (2006); A. Hesselmann, A. W. Götz, F. Della Sala, and A. Görling, J. Chem. Phys. **127**, 054102 (2007).

²⁰S. Pittalis, E. Räsänen, C. Proetto, and E. K. U. Gross, Phys. Rev. B **79**, 085316 (2009).

²¹A. D. Becke and M. R. Roussel, Phys. Rev. A **39**, 3761 (1989).

²²S. Pittalis, E. Räsänen, N. Helbig, and E. K. U. Gross, Phys. Rev. B **76**, 235314 (2007).

²³For the effective atomic units $a_0^* = (\epsilon/m^*)a_0$ and $\text{Ha}^* = (m^*/\epsilon^2)\text{Ha}$, we use the material parameters of GaAs, $m^* = 0.067m_e$ and $\epsilon = 12.4\epsilon_0$.

²⁴W.-C. Tan and J. Inkson, Semicond. Sci. Technol. **11**, 1635 (1996).

²⁵J. B. Krieger, Y. Li, and G. J. Iafrate, Phys. Rev. A **46**, 5453 (1992).

²⁶A. K. Rajagopal and J. C. Kimball, Phys. Rev. B **15**, 2819 (1977).

²⁷A. Castro, H. Appel, M. Oliveira, C. A. Rozzi, X. Andrade, F. Lorenzen, M. A. L. Marques, E. K. U. Gross, and A. Rubio, Phys. Status Solidi B **243**, 2465 (2006).